INTERNATIONAL JOURNAL OF HYDROGEN ENERGY 44 (2019) 17185–17194

Available online at www.sciencedirect.com

ScienceDirect

journal homepage: www.elsevier.com/locate/he

Palladium thin films on microfiber filtration paper as flexible substrate and its hydrogen gas sensing mechanism

Zahra Shahzamani [a], *Mehdi Ranjbar* [a,*], *Elisabetta Comini* [b], *Mehdi Torabi Goodarzi* [a], *Hadi Salamati* [a], *Giorgio Sberveglieri* [b]

[a] *Department of Physics, Isfahan University of Technology, Isfahan 84156-83111, Iran*
[b] *SENSOR, Dipartimento di Ingegneriadell'Informazione, UniversitàdegliStudi di Brescia, via Valotti 9, 25123 Brescia, Italy*

ARTICLE INFO

Article history:
Received 12 December 2018
Received in revised form
7 April 2019
Accepted 30 April 2019
Available online 24 May 2019

Keywords:
Hydrogen sensor
Sputtering
Palladium
Microfiber filtration paper
Bending

ABSTRACT

Cost-effective, simple and flexible hydrogen gas sensors operating at room temperature were demonstrated based on DC magnetron sputtered palladium thin films. The main idea is to use commercial microfiber filtration paper as a cheap, fibrous and flexible substrate for palladium. With this objective, Pd thin films with 21, 38 and 54 nm thicknesses were deposited and characterized by grazing incident X-ray diffraction (GIXRD) and scanning electron microscope (SEM). The gas sensing behavior was tested by hydrogen gas in the concentration rang of 0.5–10%. GIXRD showed a PdX/Pd phase and SEM revealed existing of many structural nanocracks. An activation process was needed where sensors were heated up to 110 °C in the presence of 10% H_2. Then a desirable hydrogen sensitivity with good stability based on hydrogen induced lattice expansion (HILE) effect in which conductance increases was observed. However, for low Pd thicknesses (21 and 38 nm) and at below 4% H_2, an inverse effect was observed in which the conductance decreased instead of increasing. For all samples the response time is incremental in the range of 0.5–4% and declining for 4–10%. Moreover, the deposited Pd sensors operate well when they are bent inward or outward. The governed physical mechanism was expressed and discussed.

© 2019 Hydrogen Energy Publications LLC. Published by Elsevier Ltd. All rights reserved.

Introduction

Today, hydrogen has become an important topic in science and technology because it is one of the future hopes for clean energy production [1–4]. However, the hazards caused by the explosion of this gas should not be ignored because of its colorlessness, being odorless, and tastelessness [5–8]. Hydrogen has a wide flammability range (4–75% in air) [9], ignition energy of 0.02 mJ [10] and can release a lot of energy (hydrogen heat combustion = 29 kcal/g) [11]. Consequently, the fabrication of low cost sensors that can detect hydrogen at low concentrations has been the subject of study by many research groups [12–15].

* *Corresponding author.*
E-mail address: ranjbar@cc.iut.ac.ir (M. Ranjbar).
https://doi.org/10.1016/j.ijhydene.2019.04.277
0360-3199/© 2019 Hydrogen Energy Publications LLC. Published by Elsevier Ltd. All rights reserved.

It has now become clear to gas sensor researchers that palladium has an extraordinary ability for sensing hydrogen [5,16–21]. It has been known that various Pd nanostructures exhibit better performance than bulk Pd. Hydrogen has high penetration rate and solubility in palladium and they react easily at room temperature [22,23]. The dissolving of hydrogen in palladium leads to formation of palladium hydride (PdH_x) which is accompanied by a change in the palladium lattice constant, and has issues such as structural expansion, structural stress and reduced electrical resistance [24]. Accordingly, depending on the degree of morphological continuity of the palladium layer, palladium based hydrogen sensors are divided into two main categories [5,25,26]. In the case of continuous Pd layers, conductance decreases due to the formation of low conductive palladium hydride. However, for a non-continues layer, the conductance may increase due to the closure of structural discontinuities across the palladium network. In this case, hydrogen sensing by palladium is based on hydrogen induced lattice expansion (HILE) effect. In contrast to conventional resistance based hydrogen sensors, the conductance in HILE effect increases due to electrical contact improvement as a result of lattice expansion caused by a phase transition to Pd hydride composition.

In fact, depending on the thickness and the morphology of the layer, these two mechanisms may coexist and compete. On the other hand, the higher the effective surface area of palladium film, the better the gas interactions and the sensing response. One of the simplest and cheapest ways to increase the effective surface area is to use porous materials as substrates in the palladium thin film deposition. So far, such substrates have been used in the preparation of palladium-based hydrogen sensors. They include alumina [27,28], silicon oxide [29], PET membranes [30], elastomeric substrates [26,31], silicon arrays [32], graphite [5], PMMA membrane [33] and nanoscale filtration membranes [34]. On the other hand, flexible substrates provide sensors that are sensitive to bending so that acting as bend sensors and can be stuck to places with various geometries. In the case of flexible substrates such as membranes and filtration papers, not only a high effective surface area is achieved due to the porosity of the substrate but also hydrogen can reach the palladium layer from the two opposite sides of the paper; the surface of the palladium layer and the back of the filter paper, which can increase the sensing response.

As an another alternative for a flexible and porous substrate, microfiber filtration papers can be used as a low cost, flexible, fibrous, porous and available support material for the fabrication of palladium thin film for hydrogen sensing purposes. The filamentous microfibers may play the role of diffusion path for H_2 molecules causing better sensing performance. Moreover, the mechanical bendability of single microfiber may prevent the Pd layers from deterioration of structural quality.

The texture of filtration papers used in our work is microfiber which has not been shown previously [35]. In the previous works, the main concerns are on the flexible or porous substrates. Many of flexible substrate, as mentioned above, lakes the good porosity and low costs. The microfiber filtration paper in this work is a cost effective flexible and porous substrate, which provides a high effective surface area for an enhanced gas absorption. In addition, most of the previous works don't show good stability over the different gas concentration or sensing cycles [31,36]. We attempt to solve this problem by an initial activation process in which removal of environmental absorbed water from the texture happens. The effect of Pd thickness on a flexible substrate is also studied in our work. To our best knowledge no report exists on sensors based on Pd layers deposited on microfiber filtration papers. So the objective of our work is to use palladium layer on this kind substrate that can detect low concentrations of hydrogen gas. We have deposited many Pd films with different thicknesses and the thicknesses reported in this work were the best choices satisfying our contribution. In this paper, thin films of palladium with of 21, 38 and 54 nm thickness were deposited on microfiber filtration papers by DC magnetron sputtering and their sensing behavior was explored. Depending on the thickness of the layer, both type of sensing mechanism including hydride formation and/or HILE effects as well as bending sensitivity are expected to be achieved. The flexible H_2 detectors will be applicable to a broad range of systems such as pipelines and mechanical components.

Materials & method

Palladium thin films were deposited on commercial filtration paper (Whatman filter paper grade 40 squares) and glass (for thickness determination) substrates using DC magnetron sputtering. Samples with different thicknesses of ($S_{21} = 21$ nm), ($S_{38} = 38$ nm) and ($S_{54} = 54$ nm) were deposited at room temperature. Argon was used as background gas and the sputtering power with voltage of 450 V and the current of 150 mA was 67.5 W. The crystalline structures were characterized using an XRD machine (Phillips XPERT with Cu-Kα radiation). The SEM analysis was performed by the Philips XL30 scanning electron microscope. The thickness of samples determined by field emission LEO 525 scanning electron microscope from Pd films deposited on glass substrate. For sensor preparation, Samples, which were cutting in 3×10 mm^2 dimensions, fixed on a support fixture by two modified Alligator Clips, these two clips worked as electrical contacts. For better contact performance, silver paste used for enhanced adhesion of paper sensor to electric pads. The Pd/filtration paper sensors were examined in a gas flow small chamber with gas inlet and outlet. Hydrogen with a flow rate of 2 l/min at various concentrations was introduced using Ar as carrier gas. An IVIUM potentiostat/galvanostat was used for measuring the conductance variation of the sensors. An activation process was performed at 10% H_2 gas under 110 °C temperature. After the activation process, the different hydrogen concentrations diluted by Argon gas, from 0.5% to 10%, were injected to test chamber with constant flow rate at room temperature. The exposure time of hydrogen injection was 3 min. A schematic drawing in Fig. 1 depicts the used test setup for activation process and gas sensing measurements. The stability of sensors was examined under 10% hydrogen exposure. To examine the effect of strain on electrical properties of sensors, current response of sensors characterized under bending inward/outward of the paper sensor. To do this, samples, cutting in 3×30 mm^2 dimensions, were

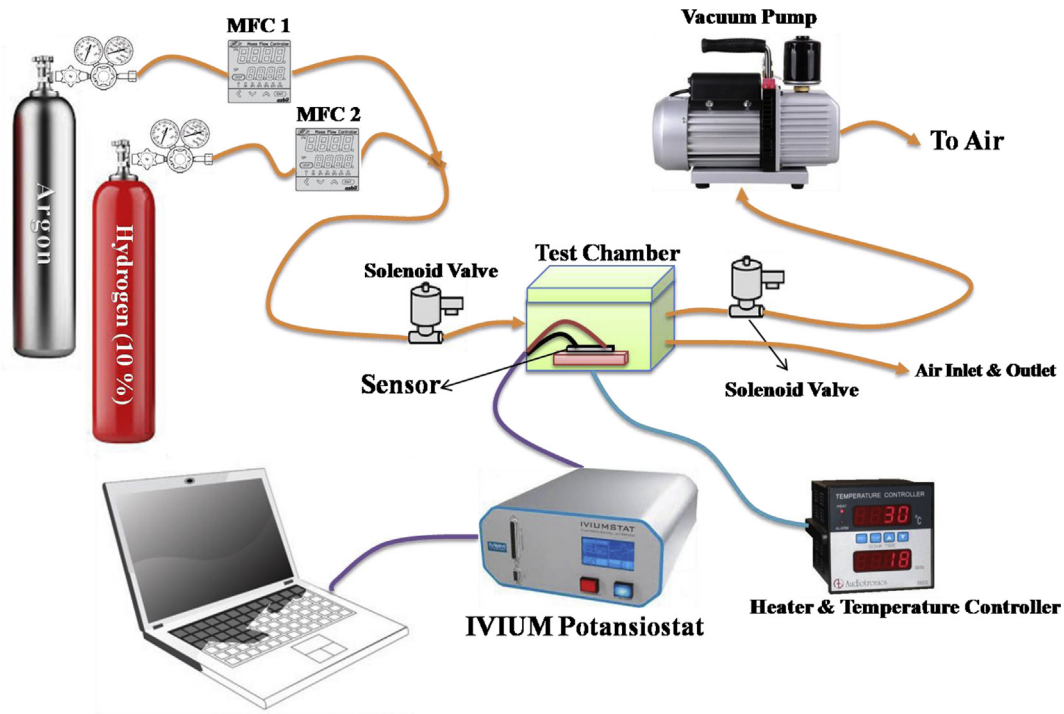

Fig. 1 – Schematic drawing of gas sensing test setup.

mounted on a computer controlled rail structure for the forward and backward movement at a specified distance. At movements, the paper sensor was bending up to 90° from unbending state and vice versa.

Results and discussion

Fig. 2 shows GIXRD analysis of Sample S_{38} as a typical sample for Pd thin film deposition on microfiber filtration paper. This pattern confirms the formation of polycrystalline cubic structure of Pd layer with preferred atomic planes of (111) and (220) that matches standard JCPDS card number 05–0681 of Pd^0. However, an additional intense peak can be found near the Pd^0 (111) which according to literature is attributed to a quasimetal phase of palladium (denoted PdX) that is forming by Oxygen insertion into the lattice of metallic palladium [37]. The presence of PdX quasimetal phase that may be due to water or oxygen molecules absorbed from the environment.

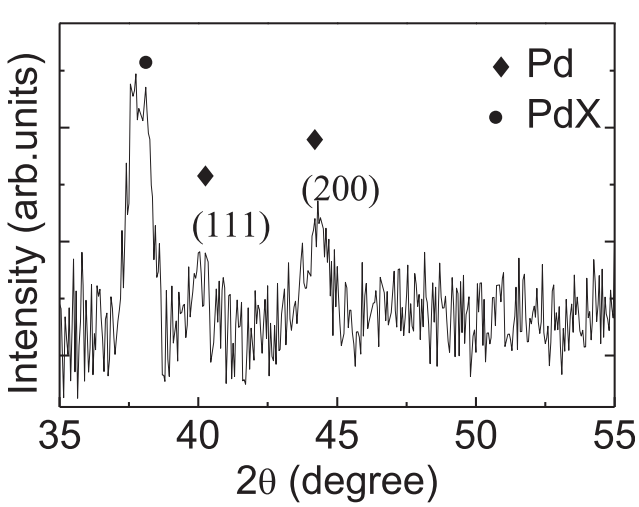

Fig. 2 – (a) GIXRD pattern of Pd thin film on microfiber filtration paper (sample S_{38}).

In this work, we kept the sputtering power constant and studied the relationship between hydrogen sensing performance and Pd thickness. After deposition, a strong layer-to-substrate adhesion was observed for the paper substrates relative to the weak adhesion on the glass, indicating that Pd films are well deposited on microfibers. Inside of Fig. 3 represents a photographic image of a deposited Pd layer on the filtration paper. Top view SEM images with different magnifications of a bare and Pd-coated paper are indicated in Fig. 3(a and b), respectively. Fig. 3(a) shows that the widths of the cellulose microfibers are around 10–50 μm. This kind of fibrous structure can provide a large specific surface area for deposited palladium that is crucial for a rapid hydrogen gas detection response. The representative SEM images with low and high magnifications after the sputter deposition of Pd layer indicates that the overall shape of the fibers and porosity are remain unchanged after deposition and Pd morphology duplicates simply that of microfibers. Nevertheless, typical cross section FESEM image of sample S_{38} deposited on glass substrate (inside of Fig. 3(b)) indicates a relatively uniform Pd layer. Comparison of high magnification SEM images in parts (a) and (b) indicates that the surface of the fibers become slightly more smooth as a result of the Pd deposition. It can be seen that the surface of cellulose fibers consists of several

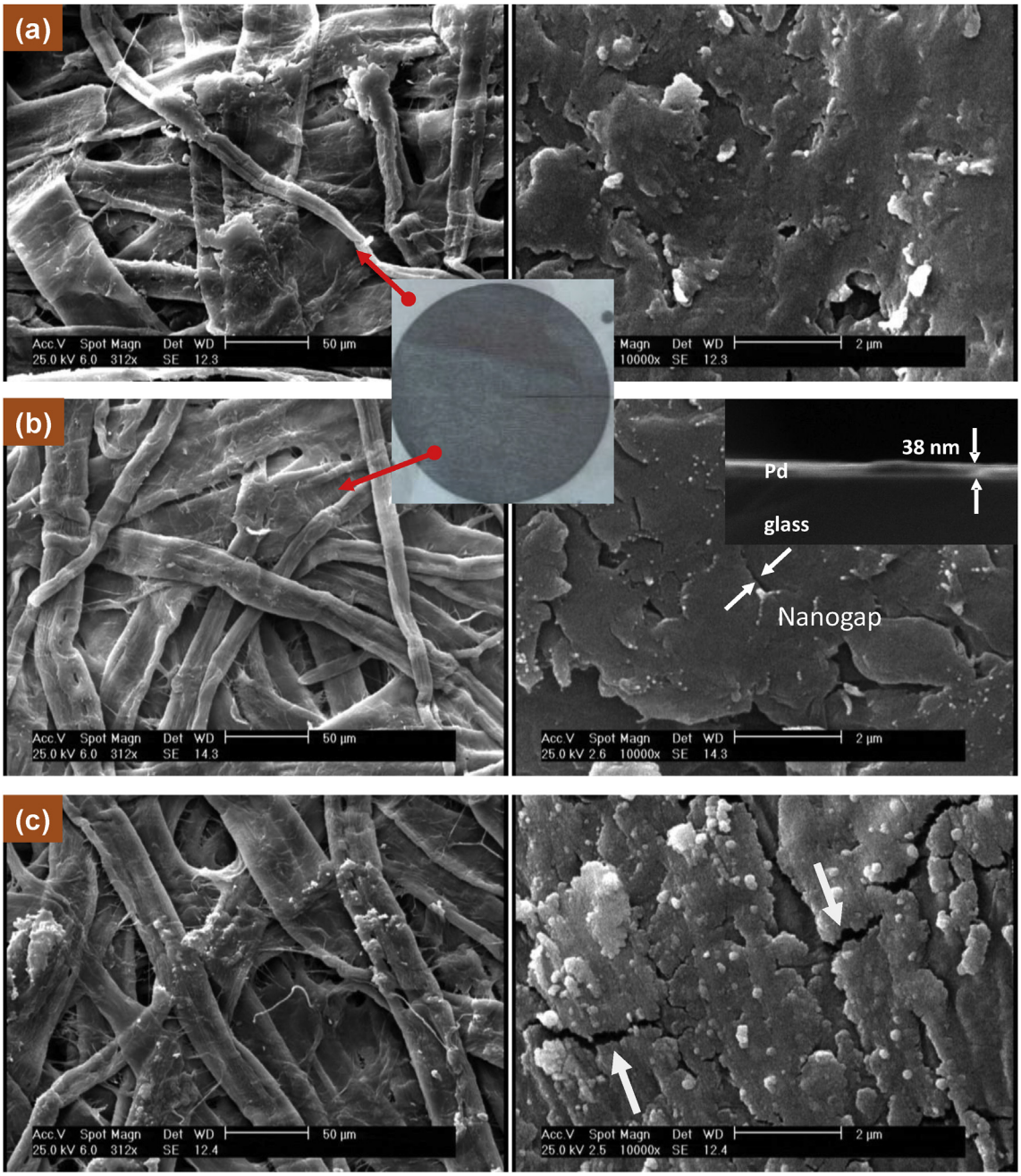

Fig. 3 – SEM images of filtration paper (a) before deposition, (b) after palladium deposition and (c) after palladium deposition and after hydrogen (10%) exposure. Inset shows a photographic image of Pd deposited filtration paper. Inside of part (b) shows cross section SEM image of Pd on glass substrate.

layered segments in which the edges and the surfaces of the segments are not uniform for bare paper. Due to Pd film growth, the crack edges become sharper and their surface smoother comparing to those observing in the bare filter paper. In addition, there are still nanometer gaps in the surface of Pd deposited samples (shown by white arrows) that can be closed by a structural expanding of PdH_x phase in the interaction with hydrogen and give rise to increase in conductance. The development of nanogaps as a result of absorption/desorption of hydrogen was investigated using SEM imaging after hydrogen exposure. SEM image in Fig. 3(c) indicates the surface of Pd-coated microfibers after hydrogen exposure. Before hydrogen exposure (part(b)), the surface of Pd layer is relatively smooth and the edges of the observable fragments are sharp. Hydrogen exposure results in surface roughening and formation of surface cracks with several nanometer scale wideness. The increase in electrical conductance and relatively fast responses will be attributed to closure of these Pd disconnections upon hydrogen exposure. Therefore, sensors fabricated by sputter deposition of Pd on

microfiber filtration paper essentially have a lot of discontinuity and are expected to exhibit the HILE effect for hydrogen sensing.

Pd thin film sensors showed some degree of conductance in zero hydrogen concentration indicating the nanogaps observed in SEM images are small and electrical connectivity is strong among the samples. To measure the electrical current of Pd-coated filtration papers for hydrogen sensing, real-time response was recorded at room temperature with various hydrogen concentrations (0.5–10%) at 2 l/min flow rate. However, before evaluation the gas sensing properties of Pd-coated filter papers, an activation process by heating samples up to 110 °C under 10% H_2 atmosphere had to be done in the first cycle. Without this process, No gas sensing was observed without activation procedure (10% H_2 at 110 °C). It was found that this initial heating is necessary for activation of the sensor performance, after which, the sensors show a desirable stability. All the samples exhibited an initial activation upon exposure to 10% hydrogen for the first time in which the conductance response increased by about 50%. Representative gas sensing cycles including the first cycle for sample S_{54} is shown in Fig. 4. As can be seen, the first cycle exhibits an irreversible increase in conductance, which is considered as the activation cycle. To give some evidences on the role of water, a typical TGA curve of filter paper coated with palladium is shown in the inside of Fig. 4. We have a weight loss between 50 and 110 °C that is attributed to water evaporation. It has been well-known that presence of water vapor affects the sensing properties by formation of PdX phase and/or preventing hydrogen dissociation on palladium [34]. The irreversible increase of conductance in the first cycle due to water evaporation can be accompanied by an irreversible stress formation due to expansion of the palladium network by the interaction with hydrogen and the formation of palladium hydride. As a result of this expansion, Pd nanocrack junctions may partially decrease the conductance. By desorbing of hydrogen from the Pd structure, the gaps of hydrogen exposed Pd films cannot return to its original state so the next baseline kept increasing. However, the effect of water desorption in the first cycle seems to overcome the reverse effect of nanogaps creation. Then the created nanogaps can be closed due to the expansion of PdH_x α and β phases in the interaction with hydrogen leading to increase in the conductance again. The subsequent cycles were performed at room temperature that are reversible so that the conductance almost recovers to the background, which can be used for sensing of various concentration of hydrogen.

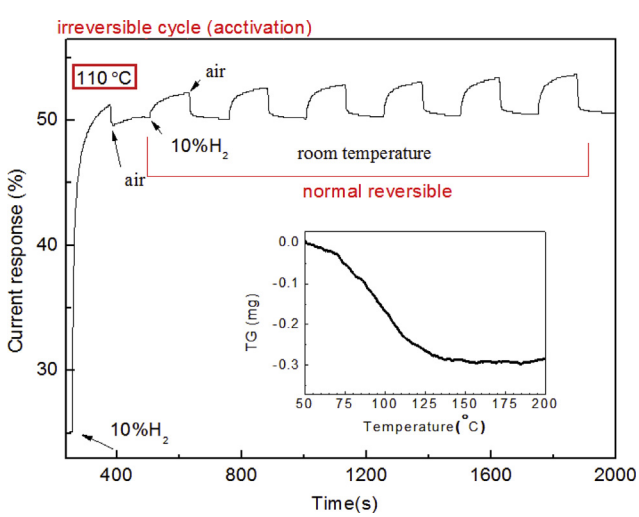

Fig. 4 – Typical sensitivity curve including first cycle as an activation stage. Inside indicates the TGA curve of sample in which a weight loss at 50–110 °C is observed due to water evaporation. In the first cycles samples are exposed to hydrogen (10%) while they are kept at 110 °C. An irreversible increase in conductance is observed.

The sensing properties were examined by exposing Pd on paper samples to various H_2 concentrations from 0.5 to 10% at room temperature. In Fig. 5(a), the response sensitivity curves are shown for S_{21}, S_{38}, and S_{54}. In Fig. 5(b), the corresponding saturation sensing signals are plotted as a function of the hydrogen concentration. It should be noted that, in Fig. 5, in contrast to Fig. 4, the responses were calculated with respect to the new baseline after activation process. Now this comment is explained in the manuscript It can be seen that samples S_{21} and S_{38} have an inverse response part in each cycle. The inverse response is more visible at low hydrogen concentrations (shown by green symbols in Fig. 5(b)) which cuts the concentration axis at a crossover point around 3–4% with a narrow dynamic range and then rise again to some positive limits. It seems that there is a competing relationship between the decrease (due to hydride formation) and increase (due to HILE effect) of conductance for sample S_{21} and S_{38}. Same results has been observed elsewhere [36] where it has been suggested that the Pd film thickness and nanogaps have opposite effects on electrical conductance of sensors. The crossover point becomes smaller as Pd thickness increases. For these two samples, the response curve (part (a)) changes to a narrow inverse peak followed by an exponential rise at H_2 concentration>4%. Although this inverse transient response is seen at higher concentrations, it seems that the positive response values are more relevant to the gas concentration. However, at low H_2 concentrations, the sensitivity with inverse values is more relevant to the H_2 concentration. So, for the lower thicknesses, both types of sensing mechanisms including hydride formation and HILE effect exist which their life time depends on the gas concentration. The hydride formation causes a mild decrease in conductance [38] so gives rise to a transient peak in response curves. Moreover, it can be seen that the absolute values of inverse responses are greater when the thickness is lower (sample S_{21}) while the positive part of signals increases with thickness. Sample S_{54}, however, has only positive responses at all the gas concentrations. The response curves versus hydrogen concentration has sigmoidal shape and values increase by palladium thickness.

In Fig. 6(a), the response time (the time required to reach 90% of the saturation of the electric current) is plotted versus the concentration of hydrogen gas for all the samples. According to this diagram, the response times of sample S_{21} is almost within 10–70 s in the 0.5–3% hydrogen concentrations range while it is about 25–130 s for sample S_{38}. In the case of sample S_{54} the response time is between 50 and 85 s in the used concentration range. For all samples, the response time

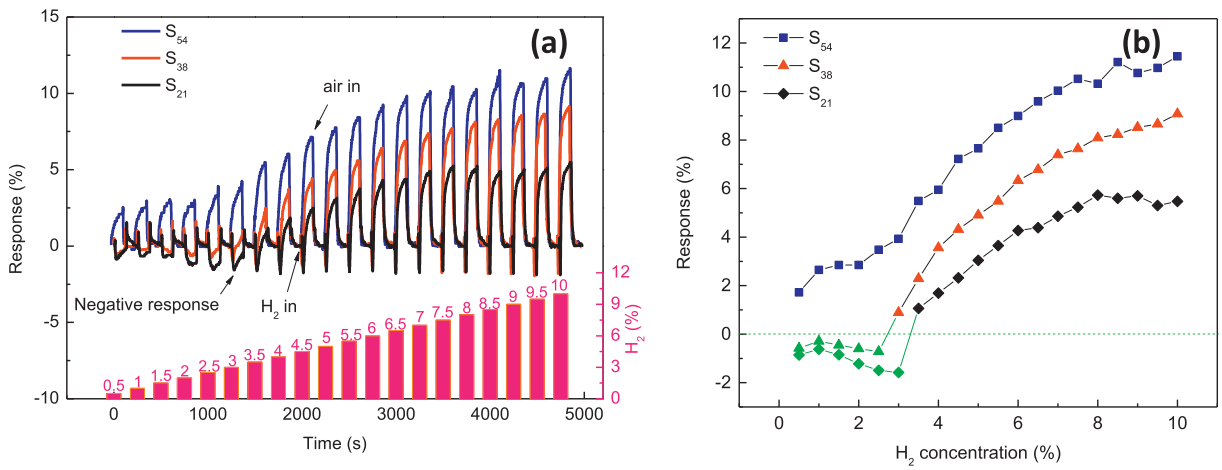

Fig. 5 – (a) Response curve of Pd/microfiber filtration papers for different Pd thicknesses at different hydrogen concentrations (0.5–10%). (b) Sensitivity as a function of hydrogen gas for different Pd thicknesses (21, 38 and 54 nm). SamplesS_{21} and S_{38} have invers (negative) response part in each cycle. There are negative response regions for samples S_{21} and S_{38} which are more visible at low hydrogen concentrations (less than 3–4% region). Sample S_{54} has only positive responses at all the concentrations.

shows a decreasing behavior above 4% H_2 concentration. In this region, the phase transition from α→β occurs, so the response time reduction can be attributed to a similar phase transition. This effect has also been reported in other papers and was attributed to PdH_x phase transition [33,39].

In order to study the repeatability of the sensors, the response of the Pd sensors with different thicknesses was measured for consecutive 37 cycles towards constant flow of the highest concentration (10% by volume) of hydrogen. These stability measurements are plotted in Fig. 7. Both hydrogen exposure and the recovery durations are 2 min. The variation of response was less than 2%. The shape and response-recovery times of the curves remain almost constant in each cycle for all samples which confirms that the samples have a desirable stability and repeatability.

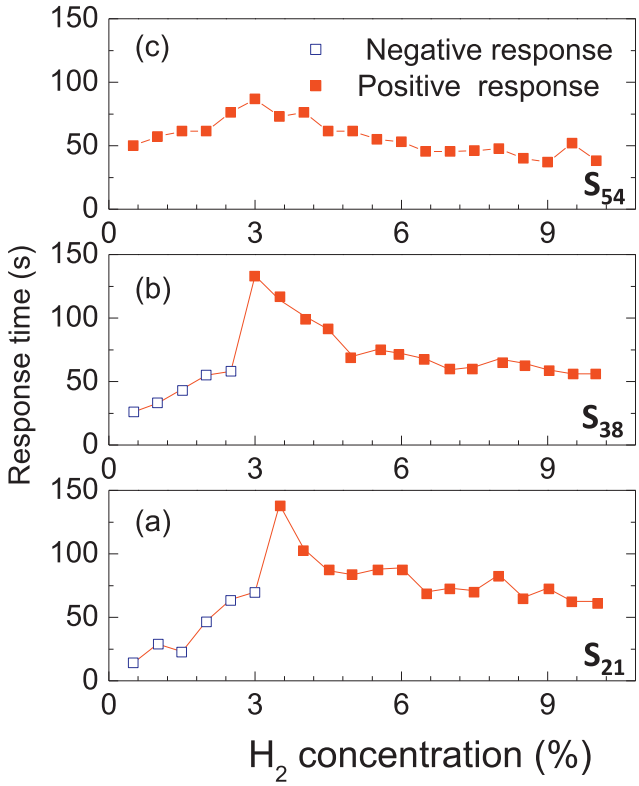

Fig. 6 – Response times (the time required to reach 90% of the saturation of the electric current) as a function of hydrogen concentration for different Pd thicknesses. For all samples, the response time decrease above 4% H_2 concentration. In this region, the phase transition from α→β occurs, so the response time reduction can be attributed to a similar phase transition.

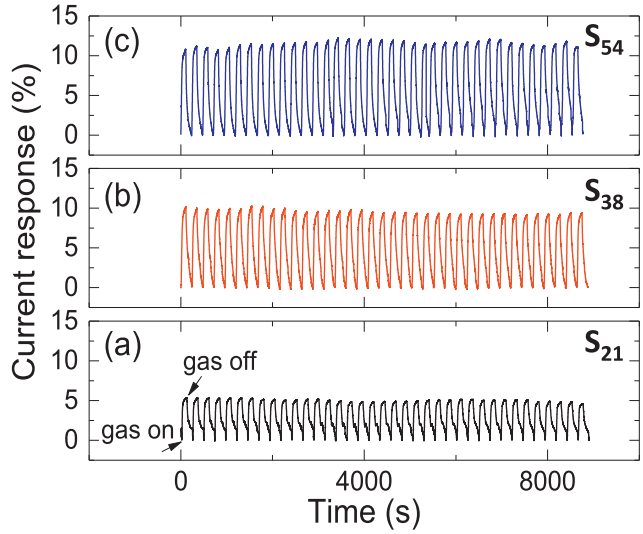

Fig. 7 – Response curves upon exposure to 10% H_2 gas at room temperature for 37 consecutive cycles, indicating repeatability and stability of the Pd sensors with different thicknesses fabricated on microfiber filtration paper. (a) S_{21}, (b) S_{38} and (c) S_{54}.

As it was mentioned above, the mechanism of increase in the conductance of Pd/microfiber filtration paper is attributed to the expansion of the palladium network and closure of nanocracks that leading to electrical connecting of existing gaps. Strain induced deformation of palladium nanocracks that were observed in SEM images (Fig. 3), is expected to have great influence on their electrical conductance similar to the effect of hydrogen exposure. Therefore, several bending tests were taken from the samples in absence and presence of gas. In Fig. 8, the electrical current response is shown for a number of bending (inward or outward) cycles for different Pd thicknesses without hydrogen exposure. As can be seen, as a result of bending, the response increases rapidly and after returning to normal states it attains the baseline. Inside of part (c) shows a comparison of electrical current of the sensor (S_{54}) for bending inward and outward. There is a significant difference between the response of the layer to the bend to the inside and outside indicating this sensor is able to detect the direction of bending. It should be noticed that a very small initial bending was required before each bending direction and this is why the unbending currents are not exactly the same. This effect can be attributed to a greater shortening of the electrical conduction paths in bending inward compared to bending outward. Therefore, the palladium on microfiber sensors are sensitive to bending so that their electrical conductance increases by bending. One can see that by increasing the palladium thickness, the current response decreases indicating that the low thicknesses provide a higher bending sensitivity.

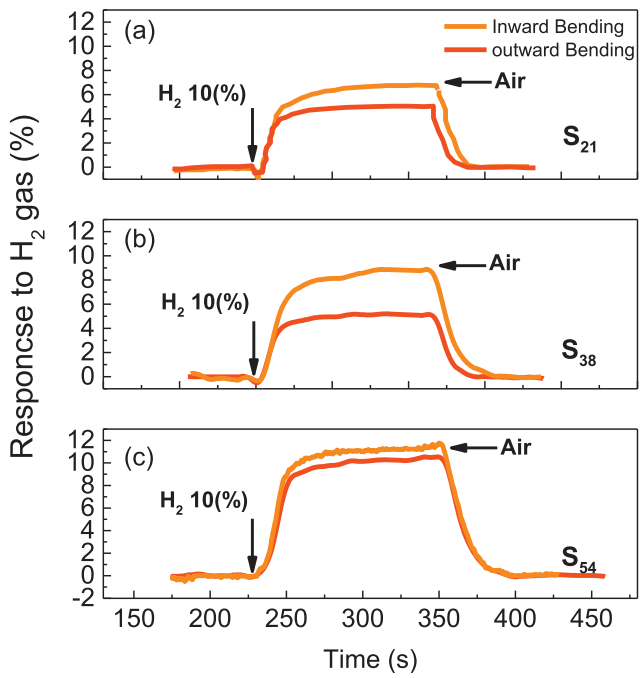

Fig. 9 – Bending response of different samples in the presence of hydrogen gas (10%) (a) S_{21}, (b) S_{38} and (c) S_{54}.

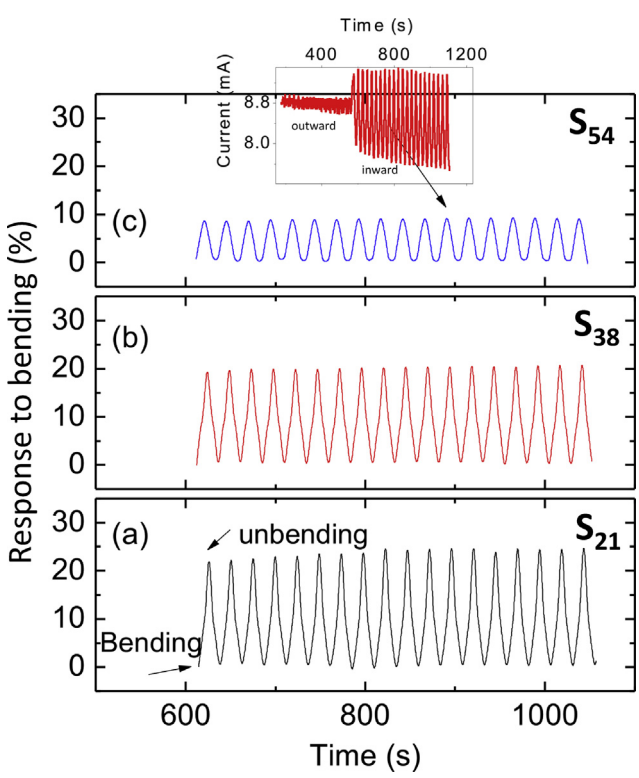

Fig. 8 – Bending response of sample for different palladium thin film samples: (a) S_{21}, (b) S_{38} and (c) S_{54}. Inset of part (c) indicates the comparison of the senor current for inward and outward bending. As can be seen, bending to inside gives higher electrical current so that it is possible to determine the direction of bending (bending sensor).

The effect of inward and outward bending on conductance change in the presence of hydrogen gas (10%) was also compared. In Fig. 9, the response of palladium sensors in one stable cycle is shown for inward and outward bending. As it can be seen, the response of the samples is greater when the Pd layers bend to the inward, rather than when they bend outward. Of course, for the thickness of 57 nm, the two responses are almost identical, and this difference is more obvious for the two low thicknesses. These observations indicate that the sensing performance of flexible Pd/paper sensors is preserved or improved at bending situations encouraging such sensors can be laminated on hydrogen leakage positions that demand mechanical durability.

The sensing mechanism can be described as follows: The adsorbed molecules on Pd are dissociated into H atoms. Then they diffuse and occupy the interstitial site of palladium lattice causing lattice expansion [40]. This process leads to palladium hydride formation and increasing of electron scattering which directly causes resistance increase of Pd layer (Fig. 10(a)). Depending on the atomic fraction of PdH_x, palladium hydride exists in three phases: α when $x < 0.015$, $\alpha+\beta$ when $0.015 < x < 0.61$ and β phase when x exceeds 0.61 at room temperature [40]. For the α phase of palladium hydride, the lattice expansion is smaller than 0.13%. There is an abrupt increase in resistance from $\alpha+\beta \rightarrow \beta$ transition which is attributed to plastic deformation of the layer. This plastic deformation is more serious for palladium thin films. Although the β phase is accompanied by an increase in conductivity, the lattice expansion role is more effective in the

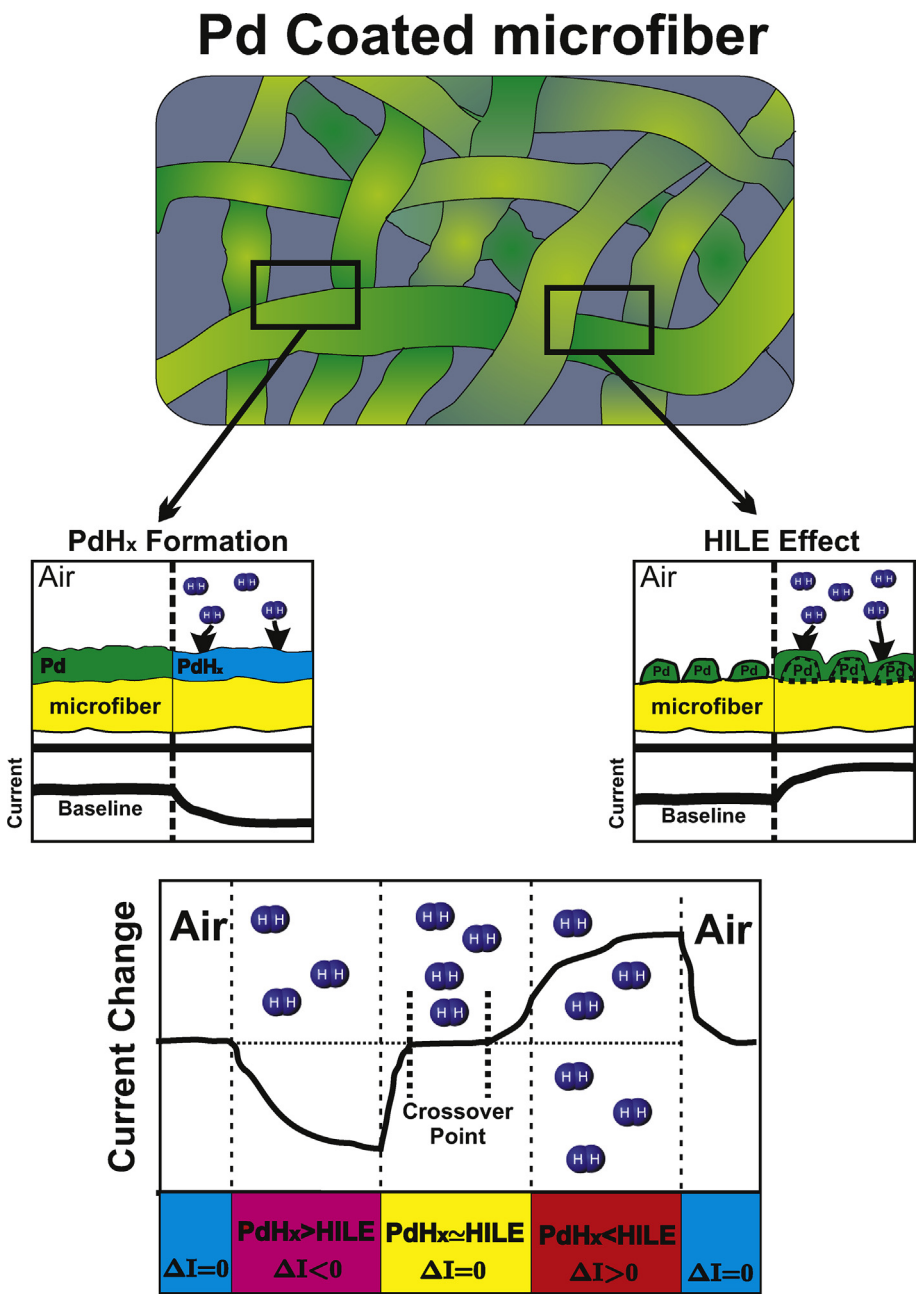

Fig. 10 – Schematic illustration of dominate mechanisms controlling the positive (a) and negative (b) responses of Pd layer.

conductivity rise due to the HILE effect. When hydrogen is removed the plastic deformation remains so we have an irreversible jump in conductance in the first cycles (Fig. 4).

The mechanism of the inverse responses observed in samples S_{21} and S_{38} can be described as follows: The morphology of the fibrous substrate consists of the crossing fibers that may be nano-spaced between them. Depending on the thickness of the palladium layer, these nanometer spaces become closer to each other after coating the Pd layer. For low thicknesses (S_{21}& S_{38}) and at low H_2concentrations (0.5–4%) only the α phase is expected to be formed, therefore the limited lattice expansion does not lead to closure of these nanometer spaces due to HILE effect. In this case, the effect of electron scattering in PdH_x across the fibers dominates the HILE effect and leads to decrease in conductivity (inverse response). By increasing the hydrogen concentration, the β phase is formed, which initially appears as an abrupt decrease in conductivity. Then the great expansion of the lattice leads to closure of all kinds of existing gaps and a monotonic increase in conductivity (Fig. 10(b)). For higher palladium thickness (S_{54}), the space between the fibers is lower so that with a slight expansion of the Pd lattice conductivity increases. This effect can be happened even in the α phase and when the expanded phase of palladium hydride is formed the connection between fibers occurs more quickly. Therefore, we assign the inverse response to formation of palladium hydride with low electrical conductance without considerable lattice expansion. By increasing hydrogen concentration, the

subsequent exponential increase in conductance is related to great Pd volume expansion due to $\alpha \rightarrow \beta$ phase transition which results in more closure of gaps and a great conductance rise (Fig. 10(c)) [38]. It is also expected that increasing the thickness is accompanied by more film tensions and increasing the layer discontinuities. Our observations suggest that when microfiber papers are used as substrate, the degree of structural deformation depends on palladium thickness and is stronger for thicker films. We observed different gas sensing mechanisms; HILE effect and PdH_x formation, which may be related to the fibrous structure of the substrate. However, this assert needs more investigation.

Conclusion

In summary, we successfully fabricated flexible palladium hydrogen sensors on commercial microfiber filtration paper using DC magnetron sputtering. Two competing sensing mechanisms were realized: a negative current response was achieved when Pd thickness and hydrogen concentration are low due to palladium hydride formation without considerable lattice expansion. Otherwise the current response is positive that is attributed to palladium hydride lattice expansion. Also, the response time of the samples depends on the concentration of gas in which a transition from an increasing to a decreasing trend was observed that was attributed to a $\alpha \rightarrow \beta$ phase transition of the PdH_x structure. These sensors are able to sense the bending and its direction. Moreover, in the presence of hydrogen gas, bending inward showed a higher sensitivity comparing to outward. This confirms the role of the expansion of the network in reducing conductivity.

REFERENCES

[1] Ni M, Leung MKH, Leung DYC, Sumathy K. A review and recent developments in photocatalytic water-splitting using TiO_2 for hydrogen production. Renew Sustain Energy Rev 2007;11:401–25.

[2] Sakintuna B, Lamari-Darkrim F, Hirscher M. Metal hydride materials for solid hydrogen storage: a review. Int J Hydrogen Energy 2007;32:1121–40.

[3] Schlapbach L, Züttel A. Hydrogen-storage materials for mobile applications. Nature 2001;414:353–8.

[4] Suh MP, Park HJ, Prasad TK, Lim DW. Hydrogen storage in metal-organic frameworks. Chem Rev 2012;112:782–835.

[5] Favier F, Walter EC, Zach MP, Benter T, Penner RM. Hydrogen sensors and switches from electrodeposited palladium mesowire arrays. Science 2001;293:2227–31.

[6] Hübert T, Boon-Brett L, Black G, Banach U. Hydrogen sensors - a review. Sensor Actuator B Chem 2011;157:329–52.

[7] Mayers B, Gates B, Yin Y, Xia Y. Functionalized carbon nanotubes for molecular hydrogen sensors. Adv Mater 2001;13:1384–6.

[8] Mor GK, Carvalho MA, Varghese OK, Pishko MV, Grimes CA. A room-temperature TiO_2-nanotube hydrogen sensor able to self-clean photoactively from environmental contamination. J Mater Res 2004;19:628–34.

[9] Miyamoto T, Hasegawa H, Mikami M, Kojima N, Kabashima H, Urata Y. Effect of hydrogen addition to intake gas on combustion and exhaust emission characteristics of a diesel engine. Int J Hydrogen Energy 2011;36:13138–49.

[10] Sherif SA, Barbir F, Veziroglu TN. Towards a hydrogen economy. Electr J 2005;18:62–76.

[11] García EY, Laborde MA. Hydrogen production by the steam reforming of ethanol: thermodynamic analysis. Int J Hydrogen Energy 1991;16:307–12.

[12] Li Z, Haidry AA, Wang T, Yao ZJ. Low-cost fabrication of highly sensitive room temperature hydrogen sensor based on ordered mesoporous Co-doped TiO_2 structure. Appl Phys Lett 2017;111.

[13] Liess M. A new principle for low-cost hydrogen sensors for fuel cell technology safety. AIP Conference Proceedings; 2014. p. 522–5.

[14] Sen A, Albarella JD, Carey JR, Kim P, McNamara III WB. Low-cost colorimetric sensor for the quantitative detection of gaseous hydrogen sulfide. Sensor Actuator B Chem 2008;134:234–7.

[15] Smith II RD, Liu P, Lee SH, Tracy CE, Pitts JR. Low-cost fiber optic hydrogen sensors. ACS Division of Fuel Chemistry, Preprints, 2 ed 2002:825–7.

[16] Mubeen S, Zhang T, Yoo B, Deshusses MA, Myung NV. Palladium nanoparticles decorated single-walled carbon nanotube hydrogen sensor. J Phys Chem C 2007;111:6321–7.

[17] Sekimoto S, Nakagawa H, Okazaki S, Fukuda K, Asakura S, Shigemori T, et al. Fiber-optic evanescent-wave hydrogen gas sensor using palladium-supported tungsten oxide. Sensor Actuator B Chem 2000;66:142–5.

[18] Sun Y, Wang HH. High-performance, flexible hydrogen sensors that use carbon nanotubes decorated with palladium nanoparticles. Adv Mater 2007;19:2818–23.

[19] Tabib-Azar M, Sutapun B, Petrick R, Kazemi A. Highly sensitive hydrogen sensors using palladium coated fiber optics with exposed cores and evanescent field interactions. Sensor Actuator B Chem 1999;56:158–63.

[20] Tobiška P, Hugon O, Trouillet A, Gagnaire H. An integrated optic hydrogen sensor based on SPR on palladium. Sensor Actuator B Chem 2001;74:168–72.

[21] Walter EC, Favier F, Penner RM. Palladium mesowire arrays for fast hydrogen sensors and hydrogen-actuated switches. Anal Chem 2002;74:1546–53.

[22] Jewell LL, Davis BH. Review of absorption and adsorption in the hydrogen-palladium system. Appl Catal Gen 2006;310:1–15.

[23] Manchester FD, San-Martin A, Pitre JM. The H-Pd (hydrogen-palladium) System. J Phase Equilibria 1994;15:62–83.

[24] Xu T, Zach M, Xiao Z, Rosenmann D, Welp U, Kwok W, et al. Self-assembled monolayer-enhanced hydrogen sensing with ultrathin palladium films. Appl Phys Lett 2005;86:203104.

[25] Pan Y-T, Yin X, Kwok KS, Yang H. Higher-order nanostructures of two-dimensional palladium nanosheets for fast hydrogen sensing. Nano Lett 2014;14:5953–9.

[26] Jang B, Kim W, Song M-J, Lee W. Thermal stability of the sensing properties in H 2 sensors composed of Pd nanogaps on an Elastomeric Substrate. Sensor Actuator B Chem 2017;240:186–92.

[27] Wu S, Zhou H, Hao M, Wei X, Li S, Yu H, et al. Fast response hydrogen sensors based on anodic aluminum oxide with pore-widening treatment. Appl Surf Sci 2016;380:47–51.

[28] Kim B-J, Kim J-S. Hydrogen sensor using the Pd film supported on anodic aluminum oxide. Int J Hydrogen Energy 2014;39:16500–5.

[29] Hu Y, Lei J, Wang Z, Yang S, Luo X, Zhang G, et al. Rapid response hydrogen sensor based on nanoporous Pd thin films. Int J Hydrogen Energy 2016;41:10986–90.
[30] Kumar R, Saraswat VK, Kumar M, Awasthi K. Palladium nanoparticle binding in functionalized track etched PET membrane for hydrogen gas separation. Int J Hydrogen Energy 2017;42.
[31] Jang B, Cho S, Park C, Lee H, Song M-J, Lee W. Palladium nanogap-based H 2 sensors on a patterned elastomeric substrate using nanoimprint lithography. Sensor Actuator B Chem 2015;221:593–8.
[32] Zhao M, Wong MH, Ong CW, Ng NH, Man HC. Tunability of Pd-nanogapped H2 sensors made on SiO2-coated Si micropillar arrays. Chemical: Sensors and Actuators B; 2017.
[33] Chen M, Mao P, Qin Y, Wang J, Xie B, Wang X, et al. Response characteristics of hydrogen sensors based on PMMA-membrane-coated palladium nanoparticle films. ACS Appl Mater Interfaces 2017;9:27193–201.
[34] Hassan K, Uddin AI, Chung G-S. Mesh of ultrasmall Pd/Mg bimetallic nanowires as fast response wearable hydrogen sensors formed on filtration membrane. Chemical: Sensors and Actuators B; 2017.
[35] Comini Elisabetta. Integration of metal oxide nanowires in flexible gas sensing devices. Sensors 2013;13:10659–73.
[36] Öztürk Sadullah, Kılınç Necmettin. Pd thin films on flexible substrate for hydrogen sensor. J Alloy Comp 2016;674:179–84.
[37] Ferhat-Hamida Z, Barbier Jr J, Labruquere S, Duprez D. The chemical state of palladium in alkene and acetylene oxidation: a study by XRD, electron microscopy and TD-DTG analysis. Appl Catal B Environ 2001;29:195–205.
[38] Zhao M, Wong MH, Ong CW, Ng NH, Man HC. Tunability of Pd-nanogapped H2 sensors made on SiO2-coated Si micropillar arrays. Sensor Actuator B Chem 2018;255:944–51.
[39] Zeng X, Latimer M, Xiao Z, Panuganti S, Welp U, Kwok W, et al. Hydrogen gas sensing with networks of ultrasmall palladium nanowires formed on filtration membranes. Nano Lett 2010;11:262–8.
[40] Noh J-S, Lee JM, Lee W. Low-dimensional palladium nanostructures for fast and reliable hydrogen gas detection. Sensors 2011;11:825–51.